THE JOURNAL OF PHYSICAL CHEMISTRY B
A JOURNAL OF THE AMERICAN CHEMICAL SOCIETY

pubs.acs.org/JPCB

Perspective

Peptide Self-Assembly into Amyloid Fibrils: Unbiased All-Atom Simulations

Bradley L. Nilsson,* Gizem Celebi Torabfam, and Cristiano L. Dias*

Cite This: https://doi.org/10.1021/acs.jpcb.3c07861

Read Online

ACCESS | Metrics & More | Article Recommendations

ABSTRACT: Protein self-assembly plays an important role in biological systems, accounting for the formation of mesoscopic structures that can be highly symmetric as in the capsid of viruses or disordered as in molecular condensates or exhibit a one-dimensional fibrillar morphology as in amyloid fibrils. Deposits of the latter in tissues of individuals with degenerative diseases like Alzheimer's and Parkinson's has motivated extensive efforts to understand the sequence of molecular events accounting for their formation. These studies aim to identify on-pathway intermediates that may be the targets for therapeutic intervention. This detailed knowledge of fibril formation remains obscure, in part due to challenges with experimental analyses of these processes. However, important progress is being achieved for short amyloid peptides due to advances in our ability to perform completely unbiased all-atom simulations of the self-assembly process. This perspective discusses recent developments, their implications, and the hurdles that still need to be overcome to further advance the field.

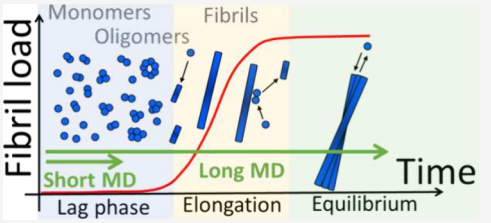

Downloaded via UNIV OF ROCHESTER on March 7, 2024 at 15:31:37 (UTC).
See https://pubs.acs.org/sharingguidelines for options on how to legitimately share published articles.

INTRODUCTION

The self-assembly of peptides and proteins into cross-β-amyloid aggregates is a characteristic of both amyloid protein folding disorders and regulated assembly of functional structures in biological systems.[1−4] Cross-β-amyloid fibrils are composed of parallel or antiparallel β-sheets in which the amide carbonyl and N−H groups are oriented parallel to the fibril axis, enabling formation of intermolecular stabilizing hydrogen bonds between neighboring peptides within a β-sheet.[5,6] The side chain groups are oriented perpendicular to the β-sheets, facilitating cross-sheet side chain interactions that also stabilize the assembled systems. Multiple β-sheets are typically laminated to give rise to the observed fibril structures.

The mechanisms of cross-β-amyloid self-assembly are the focus of intense research interest.[7,8] Amyloid self-assembly is a nucleation-dependent process characterized by an initial nucleation phase, during which prefibrillar oligomeric aggregates are formed, followed by an exponential growth phase wherein nuclei mature into fibrils by addition of monomer. Experimental kinetic and thermodynamic analyses have provided insight into these self-assembly processes, although the events that occur during the nucleation phase remain poorly understood.[9,10] These events are of particular importance in disease-relevant amyloid self-assembly since data indicates that prefibril oligomers may be the main toxic congeners in the related disorders.[11,12] The direct characterization of these early amyloid intermediates is challenging. Thus, computational simulations have proven to be a critical tool to gain insight into early events during the self-assembly process.[13,14] This perspective discusses recent advances in the use of unbiased all-atom simulations in the interrogation of early amyloid self-assembly events.

Diversity of Amyloid Fibril Structures. The kinetics of amyloid self-assembly and the structures formed during this process differ significantly for short (<10 residues) and long (>30 residues) peptides. In amyloid fibrils, each short peptide is incorporated onto one β-sheet, whereas in fibrils of long peptides, different segments along the sequence form unique β-sheets separated from each other by β-arc loop regions,[15] see Figure 1a and 1b. These β-sheets are more often (but not always) parallel for long peptides, whereas they are more variably parallel or antiparallel for short peptides depending on their amino acid sequence. Two or more β-sheets pack against each other in laminates to bury nonpolar side chain residues away from the solvent, accounting for the characteristic cross-β-pattern of amyloid fibrils.[16] For short peptides, Eisenberg and Sawaya[15] identified six and four symmetry classes that emerge from packing of parallel or antiparallel β-sheets against each other, respectively, see Figure 1c and 1d. Recently, polymorphic cross-β-structures of the amphipathic $(FKFE)_2$ peptide determined by cryo-EM have been reported in which the laminated β-sheets are of differing orientations, one parallel and one antiparallel,[17] suggesting the existence of additional

Received: November 30, 2023
Revised: February 16, 2024
Accepted: February 20, 2024

ACS Publications © XXXX American Chemical Society

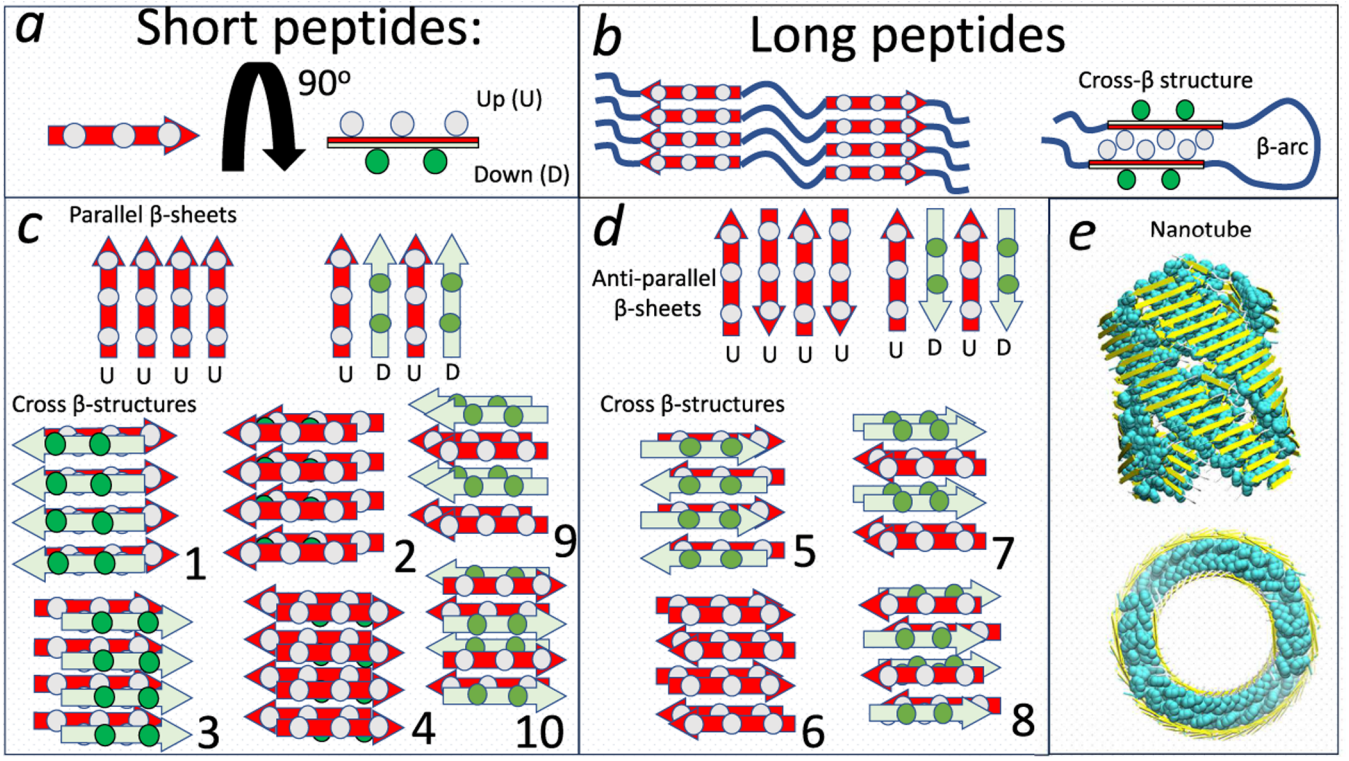

Figure 1. Cross-β-structures from short and long peptides. (a) Short amyloid peptides fold into β-strands where side chains can point in one of two directions labeled up and down. They can form (c) parallel and (d) antiparallel β-sheets with all up side chains pointing in the same direction or where up and down side chains alternate. Six and four types of cross-β structures (or symmetry classes) can be formed by laminar packing of parallel and antiparallel β-sheets. Numbers close to the different cross-β-structures refer to the symmetry classes identified by Eisenberg and Saway.[15] (e) Thin nanotube (PDB ID: 7LQG) formed by packing four fibrils from $(FKFE)_2$ peptides.[17] (b) Schematic representation of a cross-β-structure and β-arc in long peptides.

symmetry classes, see Figure 1e. Currently, it remains unclear how a single peptide sequence can form different types of β-sheets in these self-assembled structures.

Amyloid peptides require a minimum critical concentration to form fibrils, and there is evidence that disordered globular aggregates emerge at high concentrations without nucleating fibrils within experimental time scales.[18,19] This upper bound concentration is dependent on the peptide sequence and is on the order of a few millimolar for the long Aβ peptide, whereas it may be much higher or lower for short peptides. This is relevant for computational studies since all-atom simulations cannot track the motion of more than a few millions of atoms for a few microseconds using state-of-the-art resources. This accounts for simulations in which the peptide concentration is usually above the upper critical concentration of long peptides.[20]

Amino Acid Sequences of Short Amyloid Peptides. Experimentally, short amyloid peptides rapidly form fibrils at concentrations that are accessible to all-atom simulations.[14,21,22] The amino acid sequence of these short peptides often corresponds to small amphipathic segments of longer pathological amyloids. This includes segment 16−22 of the Aβ peptide (KLVFFAE) and segment 23−27 of amylin (FGAIL). These segments play an important role in triggering the aggregation of the corresponding full-length amyloid peptides, and thus, understanding their self-assembly (through simulations and experiments) may have implications for the self-assembly processes and the treatment of related diseases by perturbing these processes.[23] Extensive efforts are also being dedicated to the design of nontoxic short amyloid-like peptides for biotechnological applications. The latter efforts often take advantage of aromatic amino acids (e.g., phenylalanine and tyrosine) that are found with higher probability in sequences that form fibrils.[24] The distribution of polar and nonpolar amino acids in the peptide sequence is also a main consideration in these initiatives.[25] Cases in point are sequences with alternating nonpolar and polar amino acids which favor the formation of extended conformations where hydrophobic and hydrophilic side chains are segregated to different β-sheet faces. This facilitates burial of nonpolar residues in cross-β-structure formation. Examples of the latter sequences include EAK16-II (AEAEAKAKAEAEAKAK),[26] $(FKFE)_2$,[27] and RAD16-I (RADARADARADARADA)[28] peptides.

Nowadays, it is mostly accepted that the formation of amyloid fibrils emanates from the general properties of the polypeptide backbone.[29] Thus, any peptide sequence is expected to form fibrils under the appropriate conditions, although off-pathway oligomers have also been reported.[30,31] However, the propensity of a peptide to form fibrils depends enormously on its amino acid sequence. The latter determines the secondary structure of peptides and their ability to segregate nonpolar and polar residues when incorporated onto amyloid fibrils. Several of the extensive efforts to understand how the peptide sequence encodes for amyloidogenicity are now summarized in repositories like the WALTZ database.[32] The latter contains 930 hexapeptides out of which 180 form fibrils and 750 are nonamyloidogenic. This database is commonly used to develop and test bioinformatic tools aimed at guiding the design of new peptides that form fibrils.[33]

https://doi.org/10.1021/acs.jpcb.3c07861
J. Phys. Chem. B XXXX, XXX, XXX−XXX

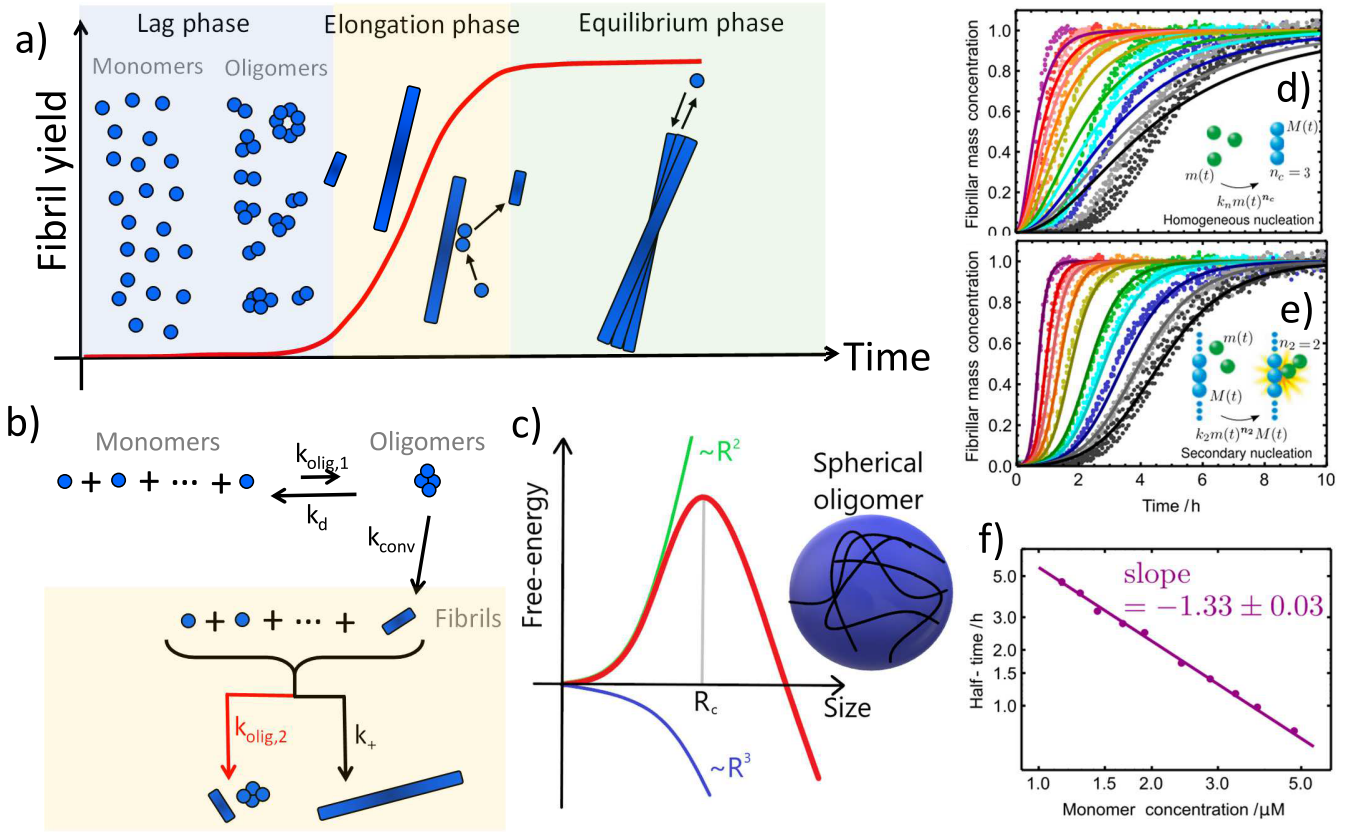

Figure 2. Kinetics of fibril formation. (a) Schematic representation of experimental fibril formation highlighting lag, elongation, and equilibrium phases. Monomers and low molecular weight oligomers coexist in the lag phase. Fibrils nucleate and grow in the elongation phase. Fibrils coexist with monomers and low molecular weight oligomers in the equilibrium phase. (b) Illustration of the different mechanisms related to fibril formation and the reaction rates associated with them. (c) Classical nucleation theories predict an energy barrier (in red) for oligomer formation. The latter emerges from the sum of an unfavorable term (in green) related to the creation of an interface with the solvent and a favorable term (in blue) associated with the formation of atomic contacts within the oligomer. (d and e) Experimental fibril yield of Aβ (dots) where each color corresponds to a different concentration ranging from 1 to 5 μM. Solid lines correspond to best fits of eqs 1−3 using (d) $k_{olig,2} = 0$ and (e) $k_{olig,2} \neq 0$. (f) Dependence of the lag phase of Aβ on peptide concentration. Reproduced from ref 51. Copyright 2013 PNAS.

The amyloid propensities of peptide sequences that differ significantly from those in the repository are, however, not always predicted correctly.[34,35] A case in point is the propensity to form fibrils of three sequences made from the same amino acids, i.e., $(FKFE)_2$, KEFFFFKE, and $(KFFE)_2$. Careful experiments have shown that $(FKFE)_2$ forms fibrils at low (0.2 mM) and high (1.0 mM) concentrations, whereas KEFFFFKE forms fibrils only at high concentration; $(KFFE)_2$ fails to form fibrils at any of the studied concentrations.[36] In contrast to all-atom simulations, existing bioinformatic tools predict a trend of aggregation for these peptides that differs significantly from the experimental observations.[21] This shows that all-atom simulations can not only provide insights into the mechanisms and structure of aggregation but also guide the design of new amyloid-like sequences.

KINETICS OF FIBRIL FORMATION

Most in vitro studies of fibril formation are carried out at fixed peptide concentrations. The assumption underlying those experiments is that peptides are initially uniformly distributed in space, and as time evolves, they aggregate into fibrils.[37] A common experiment of choice for these studies uses dyes (e.g., thioflavin-T or Congo red) that experience changes in fluorescence emission upon binding selectively to amyloid fibrils.[38] In these dye-binding assays, the fluorescence intensity can be followed as a function of time, quantifying the fibril-load increase in the system. The main goals of these studies have been to compare aggregation propensities of different proteins (e.g., wild-type versus mutated sequences) and/or compare aggregation propensities at different solvent conditions, e.g., solutions without and with inhibitors.

A characteristic fluorescence-intensity profile is shown in Figure 2a, where lag, growth, and stationary phases are highlighted.[39] The aggregates (i.e., oligomers) formed during the lag phase are made of only a handful of peptides.[40] They are mostly disordered, soluble, and unstable, whereby they dynamically disassemble into lower molecular weight species, i.e., monomers, dimers, etc. At the end of the lag phase, larger aggregates undergo a conformational change, giving rise to the fibril nucleus. Thus, it is usually assumed that fibril nucleation takes place in two steps, whereby peptides form a disordered nucleus that subsequently undergoes a conformational change, leading to ordered amyloid fibrils.[41,42] The latter elongate in the growth phase by absorbing monomers from the solution.[43,44] In the stationary/equilibrium phase, fibrils mature while coexisting with a residual number of low molecular weight species.[45]

Rate equations are often used to model fluorescence-intensity profiles.[46] Simplified versions of these equations assume that proteins exist in one of three states: monomeric,

https://doi.org/10.1021/acs.jpcb.3c07861
J. Phys. Chem. B XXXX, XXX, XXX−XXX

oligomeric, and within an amyloid fibril.[47] In this context, "oligomer" is used as an umbrella term to define nonfibrillar aggregates without needing to specify its size or configuration. Oligomers are formed at a rate $k_{olig,1}$ when monomers $m(t)$ encounter each other in solution in a process called *primary nucleation*, see Figure 2b. In classical nucleation theories, the free energy of oligomer formation emerges as the sum of favorable intermonomer interactions and an unfavorable term due to the oligomer−solvent interface.[48] Assuming spherical oligomers of radius R, former and latter terms scale as ca. $-R^3$ and R^2, respectively, accounting for the free-energy profile in Figure 2c. The latter predicts that the growth of small aggregates is unfavorable and oligomers tend to dissociate into low molecular weight aggregates at a rate k_d. Spontaneous fluctuations can, however, give rise to oligomers with larger radii. The free energy of oligomer formation is a maximum when aggregates reach the critical size R_c in Figure 2c. Accordingly, oligomers that are larger than the critical size grow favorably by incorporating monomers dissolved in solution. In the case of amyloids, large oligomers undergo a conformational change, forming protofilaments at a rate k_{conv}, see Figure 2b. These protofilaments grow irreversibly at a rate k_+ when monomers bind to its two tips in a process called fibril *elongation*. Figure 2b illustrates the different processes accounting for fibril formation that are used to write eqs 1−3 for the population of oligomers $O(t)$, concentrations of fibrils $F(t)$ in the system, and the fibril load $M(t)$.

$$\frac{dO}{dt} = k_{olig,1}m^2(t) - k_{conv}O(t)m(t) - k_dO(t) + + k_{olig,2}m(t)M(t) \quad (1)$$

$$\frac{dF}{dt} = k_{conv}O(t)m(t) \quad (2)$$

$$\frac{dM}{dt} = 2k_+F(t)m(t) \quad (3)$$

The different rates in these equations can be determined by fitting the fibril load $M(t)$ to experimental fluorescence-intensity profiles.[49] Until recently, the mechanism described by the rate $k_{olig,2}$ in eq 1 was ignored, and it will be discussed in more detail below.

Equations 1−3 have been used to study the dependence of the fibril load on the concentration of monomers. One result that emerges from these studies is that the lag phase defined by the time $t_{1/2}$ when one-half of the monomers in the solution are in the fibrillar state is given by

$$\log(t_{1/2}) = \text{constant} - \left(\frac{N_c + 1}{2}\right)\log(m) \quad (4)$$

where $\log(t_{1/2})$ depends linearly on $\log(m)$ and the slope of this equation is proportional to the number N_c of monomers in the nucleus.[46] Several experimental studies have confirmed the validity of eq 4 under certain conditions.[50,51] A case in point is shown Figure 2f for the Aβ protein.[51] Despite this success, the fibril growth velocity computed by fitting the experimental $M(t)$ to eqs 1−3 with $k_{olig,2} = 0$ is not reproduced accurately, i.e., it is much smaller than that in experiments, see Figure 2d.[51] The experimental growth velocity can only be reproduced if the last term in eq 1 is taken into account, i.e., $k_{olig,2} \neq 0$. The latter assumes that new oligomers are nucleated at a non-negligible rate on the surface of existing fibrils in solution. Thus, the last term is a function of the concentration of monomers (i.e., $m(t)$) and the concentration of proteins in the fibrillar state, i.e., $M(t)$. This mechanism of nucleation on the fibril surface is known as *secondary nucleation*, and it enables eqs 1−3 to provide a reasonable description of experiments as shown in Figure 2e.[51,52]

Rate constants obtained by fitting eqs 1−3 to experiments have provided important insights into the different mechanisms accounting for fibril formation.[47] Whereas the first fibrils in the system have to emerge via primary nucleation, most subsequent fibrils were found to emerge from oligomers formed via a secondary nucleation mechanism. Moreover, oligomers were found to be mostly unstable and to dissociate into monomers with only a very small fraction of them being converted into fibrils. This accounts for a more holistic view of amyloid formation where there is a strong interdependence of monomer, oligomer, and fibril populations. Thus, it is not possible to predict the concentration of oligomers (which are the toxic aggregates in many amyloid diseases) without knowledge of fibril and monomer populations.

■ ALL-ATOM SIMULATIONS

All-atom simulations have the potential to provide insights into the pathways and interactions accounting for the different mechanisms enabling fibril formation.[14] This knowledge is critical to correlate amyloid self-assembly with emergent amyloid toxicity in protein folding disorders and to potentially enable the rational design of drugs to treat amyloid diseases by selectively perturbing formation of toxic oligomeric species without disrupting nontoxic species, including fibrils.[53] In long simulations performed with a few thousand molecules of protein at a concentration of ∼1 μM, one would expect to see the first fibrils emerging via primary nucleation. The latter would then grow via monomer addition while catalyzing the formation of oligomers on its surface. Most of these oligomers would dissociate into monomers, and only a few of them would form new fibrils. Alternatively, these types of simulations may also indicate that oligomer formation and fibril formation pathways are separate, requiring disassembly of intermediates in order to move from oligomeric pathways to fibril formation pathways. Since the coordinates of all of the atoms are known in these simulations, it would be possible to determine the interactions accounting for primary and secondary nucleation as well as fibril growth. However, this holistic picture remains impossible to simulate using all-atom models in explicit solvent as it requires tracking a large number of atoms (i.e., $\sim 10^{11}$ atoms if 1000 peptides are simulated at a concentration of 1 μM) for many time steps (e.g., $\sim 10^{12}$ time steps to account for 1 ms).

An alternative approach has been to simulate a few peptides in solvated boxes at concentrations greater than 1 mM. Enhanced sampling methods are commonly used to obtain converged structures of monomers from full-length amyloid peptides.[54] These structures are affected by point mutations,[55] conditions of the solvent, e.g., the presence of salts and inhibitors,[56] but also the choice of force field used to perform the simulation.[55,57] In the case of Aβ(1−42), a strand−loop−strand conformation[58−60] has frequently been associated with an intermediate state on the pathway to fibril formation wherein residues 26−32 adopt a looplike structure enabling residues 16−22 to form a β-sheet with residues 38−42.[55,56] The *Venetian blind* pathway of fibril formation suggests that nucleation emerges from the juxtaposition of two strand−

https://doi.org/10.1021/acs.jpcb.3c07861
J. Phys. Chem. B XXXX, XXX, XXX−XXX

loop−strand structures followed by the rotation of the strands wherein intrapeptide hydrogen bonds are replaced by interpeptide bonds.[61] In contrast to strand−loop−strand structures, the formation of a β-sheet involving three strands (residues 16−22, 26−32, and 38−42) could slow down or impede the formation of fibrils.[56] Despite these insights, the complete process ending up in the formation of cross-β-structures for full-length amyloid has only be simulated using coarse-grained simulations.[62,63]

All-atom simulations of short fragments of amyloid peptides have mostly provided insights into the formation of disordered aggregates. Recent studies however show that these disordered aggregates also form fibrils if simulations are performed long enough using the appropriate force fields. In particular, the Aβ(16−22) peptide was shown to form fibrils within a time frame of 2 μs using variants of the CHARMM36m force field, whereas fibrils did not form successfully using AMBER99SB-disp.[22,64] In another study, the amphipathic $(FKFE)_2$ peptide was shown to form a fibril using the AMBER99SB-ildn force field, and at high peptide concentrations, increasing temperature was shown to accelerate this process.[21] In the same vein, simulations with a preformed fibril and a few peptides randomly located in the simulation box were used to study fibril growth[65−67] and secondary nucleation.[65] These studies are opening the door to our understanding of the sequence of molecular events leading to fibril formation.

Primary Nucleation. Using a multiscale method, primary nucleation of Aβ(16−21) peptides was shown to emerge in one or two steps depending on whether a disordered nucleus formed before the fibril-like state.[42] The absence of a disordered nucleus was observed preferentially at submillimolar concentrations, whereas ordered β-sheets emerged from the core of a disordered nucleus at high concentrations. These results are consistent with all-atom simulations of the amphipathic $(FKFE)_2$ peptide where cross-β-structures formed in the presence of a disordered nucleus (at the highest concentrations studied) and in the absence of a disordered nucleus (at the lowest concentrations studied).[65] In both pathways, the two β-sheets of the cross-β-structure were initially oriented perpendicularly to each other, see blue panel in Figure 3. This intermediate structure was shown to last for at least ∼0.5 μs before these β-sheets rotated to become aligned with each other, enabling additional growth. Hydrophobic interactions and hydrogen bonds were shown to stabilize this intermediate state. If these perpendicular cross-β-structures are found to be general intermediate states on the pathway to fibril formation, they could become a target for agents to inhibit fibril formation. This could have important implications to treat amyloid diseases.

In the near future, we anticipate that extensive all-atom simulations will be performed to understand the relation between peptide sequence and fibril formation. This will provide (i) more accurate predictions of peptides that can form amyloid fibrils, (ii) an outline of the different pathways leading to the formation of cross-β-structures and how these pathways depend on the peptide sequence, and (iii) an understanding of how different nanofibril morphologies are related to the peptide sequence. Although this level of understanding remains mostly unknown, the striking effect of the peptide sequence on the formation of cross-β-structures can be highlighted by comparing coarse-grained simulations performed using the OPEP force field for the $(KFFE)_1$ peptide[68] with all-atom simulations of $(FKFE)_2$ peptides.[21] In the former simulations,

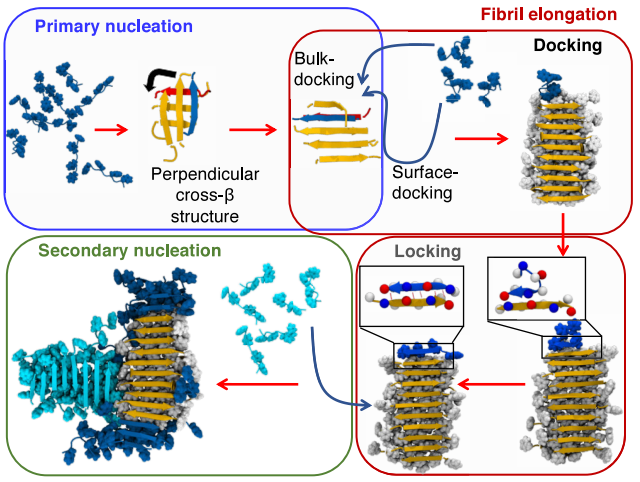

Figure 3. Schematic illustration of the mechanisms accounting for fibril growth. (Blue panel) Primary nucleation takes place with peptides aggregating in solution to form an intermediate cross-β structure where β-sheets are oriented perpendicularly to each other. (Red panels) Fibril elongation takes place via a dock-and-lock mechanism. Peptides populate the fibril tip either after performing a random walk in solution (i.e., bulk-docking) or after being directed toward it after landing on the fibrils surface, i.e., surface-docking. After landing on the fibril tip, side chains drive the proper alignment of peptides with the fibril, i.e., locking. (Green panel) Hydrophobic patches on the fibril surface enable the nucleation and account for the orientation of new fibrils via secondary nucleation. Reproduced from ref 65. Copyright 2024 American Chemical Society.

aggregation proceeded bidirectionally along both the main axis of the β-sheet and the stacking of different layers of β-sheets on top of each other. In contrast, $(FKFE)_2$ peptides in all-atom simulations aggregated unidirectionally along the main axis of β-sheets while forming a perpendicular cross-β-structure intermediate.[21]

Fibril Elongation. Simulations of preformed fibrils with peptides dispersed in solvated boxes can be used to study how peptides become incorporated onto the fibril ends accounting for its elongation.[69] Recently, it was shown that this type of simulation can be performed without biases.[65] In particular, atomic restrains are not required to stabilize the preformed fibril, and peptides can elongate the fibril independently of initial molecular positions. In these simulations, elongation proceeds via the commonly accepted dock-and-lock mechanism, whereby peptides promptly land onto the fibril tip in a random conformation (dock phase) before slowly adopting the structure dictated by the fibril tip (lock phase).[69] It is often assumed that peptides land on the fibril tip after diffusing in solution, i.e., bulk-docking. However, this assumption is almost never tested as most simulations are performed starting with peptides already docked onto the fibril tip.[70] Unbiased simulations are showing that peptides can also populate the fibril tip after diffusing on the fibril surface, i.e., surface docking,[65] see upper red panel in Figure 3. The latter pathway was shown to contribute significantly to docking.[66]

There is a long-standing debate about how docked peptides adopt the structure established by the fibril tip.[44,71] The mechanism giving rise to this locking process is expected to be robust since, for a micrometer-long fibril, it is reproduced by more than 1000 peptides with atomic precision. Proposed mechanisms for locking include a random conformational search of docked peptides until they adopt the locked structure

https://doi.org/10.1021/acs.jpcb.3c07861
J. Phys. Chem. B XXXX, XXX, XXX−XXX

(i.e., *random templating* mechanism) and a conformational search driven by side chain interactions, i.e., *driven templating*. Both mechanisms have been studied theoretically and using coarse-grain models.[44,71] In recent unbiased all-atom simulations using the $(FKFE)_2$ peptide, temperature was used as a parameter to increase the randomness of the conformational change.[65] In seven independent simulations performed at high (350 K) temperatures, docked peptides locked themselves in "imperfect" conformations, e.g., in an parallel β-sheet structure instead of the expected antiparallel one. These "imperfectly-locked" peptides were stable until the end of the simulation and for almost 1 μs. In contrast, docked peptides adopted the structure imposed by the fibril tip at 325 K. This emerged in a stepwise manner wherein complementary charged side chains at one extremity of the peptide became aligned first followed by the other extremity, see lower red panel in Figure 3. Thus, all-atom simulations for the $(FKFE)_2$ peptide suggest that locking proceeds via a template-driven mechanism instead of random templating.

Secondary Nucleation. Enhanced sampling simulations of Aβ peptides have shown that secondary nucleation is driven by the release of a large number of water molecules to the bulk, enabling the formation of nonpolar interactions between the peptides and the fibril.[72] The importance of hydrophobic interactions was also highlighted using Discrete Molecular Dynamics simulations of the heterogeneous aggregation of Aβ(1−40) peptides on the surface of fibrils from Aβ(16−22).[73] In implicit solvent simulations, the diffusion of peptides on the fibril surface (see surface-docking pathway in fibril elongation[65]) allowed Aβ peptides to encounter each other on the surface.[74] The latter events could lead to secondary nucleation.

More recently, secondary nucleation was also studied using unbiased all-atom simulations of short $(FKFE)_2$ peptides,[65] see Figure 3. In these simulations, adsorbed monomers were shown to diffuse and detach from the fibril surface but not dimers or higher order aggregates, which remained bound to the fibril surface for the whole duration of the simulation. Secondary nucleation started with monomers or dimers landing on the fibril surface where they adopted extended conformations to maximize nonpolar interactions with the fibril. This facilitated the formation of β-sheets, dictating their orientations with respect to nonpolar patches on the fibril surface, see green panel in Figure 3. The nonpolar pattern on the surface may therefore template the formation of new fibrils during secondary nucleation events, propagating specific fibril structures/strains.[52]

OUTLOOK

In this perspective, we have discussed recent developments showing that unbiased all-atom simulations can be used to study not only the formation of disordered aggregates but also the formation of ordered cross-β-structures from small peptides. The importance of these developments is compounded by advances in experimental methods (e.g., cryo-EM, 2D IR spectroscopy, and solid-state NMR) that can determine not only the hydrogen-bond registry of peptides in β-sheets but also the packing of these sheets into cross-β-structures and larger scale structures, e.g., nanotubes and nanoribbons.[5,17,75] We anticipate that these experimentally resolved structures will be used to improve current force fields, which in turn will be used to make new structural predictions that can be tested. Although current force fields can fold a large number of protein sequences into a variety of different structures, some studies are showing that they do not capture experimentally observed residue-specific conformational propensities of short GxG peptides (where x is the residue of interest) in water.[76] The latter was confirmed for two six-residue peptides with motif RxxS.[77] In the same vein, protein−protein interactions appear to be overestimated in most force fields compared to protein−water interactions.[78] Thus, a feedback loop between experiments and simulations is needed to improve our understanding of peptide self-assembly, which is one of the open challenges in physical chemistry.

The novel long trajectories generated using unbiased all-atom simulations are also providing opportunities for developments of new order parameters that are needed not only to account for the diversity of cross-β structures (see Figure 1) but also to characterize larger scale structures made by combining various fibrils.[22,79] This will allow the development of a framework to understand how mesoscopic structures of nanofibrils emerge from interactions at the atomic level. Therefore, the search for complex order parameters may become an intensive area of research in the theoretical physical chemistry community. Although this perspective focuses on unbiased all-atom simulations, we would be remiss not to mention the important role played by coarse-grained simulations in describing phenomena taking place at longer and larger length scales[80−83] or the role played by alpha-fold.[84] It is also anticipated that our understanding of amyloid aggregation will be significantly improved by studying longer model peptides, which exhibit β-arcs in the fibril state, see Figure 1e. These peptides adopt a broader spectrum of conformations compared to the less than 10-residue peptides discussed in this perspective. Currently, it has not been possible to simulate fibril formation from longer peptides, and it remains an open question of whether the current force fields need to be modified to account for the formation of beta-arcs.

AUTHOR INFORMATION

Corresponding Authors

Bradley L. Nilsson − *Department of Chemistry, University of Rochester, Rochester, New York 14627-0216, United States; Materials Science Program, University of Rochester, Rochester, New York 14627-0216, United States;* orcid.org/0000-0003-1193-3693; Email: bradley.nilsson@rochester.edu

Cristiano L. Dias − *Department of Physics, New Jersey Institute of Technology, Newark, New Jersey 07102-1982, United States;* orcid.org/0000-0002-8765-3922; Email: cld@njit.edu

Author

Gizem Celebi Torabfam − *Department of Physics, New Jersey Institute of Technology, Newark, New Jersey 07102-1982, United States;* orcid.org/0000-0002-4985-3632

Complete contact information is available at: https://pubs.acs.org/10.1021/acs.jpcb.3c07861

Notes

The authors declare no competing financial interest.

https://doi.org/10.1021/acs.jpcb.3c07861
J. Phys. Chem. B XXXX, XXX, XXX−XXX

Biographies

Bradley L. Nilsson is a Professor of Chemistry at the University of Rochester. He earned his Ph.D. degree in Organic Chemistry at the University of Wisconsin−Madison and conducted postdoctoral studies at the University of California, Irvine. He joined the faculty of the Department of Chemistry at the University of Rochester in 2006. The Nilsson group is interested in supramolecular chemistry with a focus in amyloid self-assembly and the exploitation of self-assembling peptides in the design of novel biomaterials.

Gizem Celebi Torabfam is a visiting Ph.D. student in the Material Science Program at New Jersey Institute of Technology. She has a B.Sc. degree in Molecular Biology and Genetics from Istanbul Technical University, Turkey, and an M.Sc. degree in Genetics from Istanbul University, Turkey. Her research interests include biophysics and molecular biology.

Cristiano L. Dias is an Associate Professor in the Department of Physics at the New Jersey Institute of Technology (NJIT). He received his Ph.D. degree in Physics from McGill University and worked as a postdoctoral fellow at Western University, University of Toronto, and Freie Universität Berlin. The focus of the Dias lab is in understanding self-assembly processes in bulk solution and water−lipid interfaces related to human health.

■ ACKNOWLEDGMENTS

C.L.D. would like to thank Sharareh Jalali and Yanxing Wang for insight discussions. This work was supported by the National Science Foundation under Grant Nos. CHE-2304853 and CHE-2304852 and by the National Institute of General Medical Health under Grant No. 1R15GM148982-01.

■ REFERENCES

(1) Dobson, C. M.; Knowles, T. P. J.; Vendruscolo, M. The Amyloid Phenomenon and Its Significance in Biology and Medicine. *Cold Spring Harbor Perspectives in Biology* **2020**, *12*, a033878.
(2) Ke, P. C.; Sani, M.-A.; Ding, F.; Kakinen, A.; Javed, I.; Separovic, F.; Davis, T. P.; Mezzenga, R. Implications of peptide assemblies in amyloid diseases. *Chem. Soc. Rev.* **2017**, *46*, 6492−6531.
(3) Buchanan, J. A.; Varghese, N. R.; Johnston, C. L.; Sunde, M. Functional Amyloids: Where Supramolecular Amyloid Assembly Controls Biological Activity or Generates New Functionality. *J. Mol. Biol.* **2023**, *435*, 167919.
(4) Myers, C.; Cornwall, G. A. Host defense amyloids: Biosensors of the immune system. *Andrology* **2023**, 1−8.
(5) Jaroniec, C. P. Two decades of progress in structural and dynamic studies of amyloids by solid-state NMR. *J. Magn. Reson.* **2019**, *306*, 42−47.
(6) Fitzpatrick, A. W.; Saibil, H. R. Cryo-EM of amyloid fibrils and cellular aggregates. *Curr. Opin. Struct. Biol.* **2019**, *58*, 34−42.
(7) Michaels, T. C. T.; Qian, D.; Šarić, A.; Vendruscolo, M.; Linse, S.; Knowles, T. P. J. Amyloid formation as a protein phase transition. *Nature Reviews Physics* **2023**, *5*, 379−397.
(8) Zhang, Z.; Huang, G.; Song, Z.; Gatch, A. J.; Ding, F. Amyloid Aggregation and Liquid−Liquid Phase Separation from the Perspective of Phase Transitions. *J. Phys. Chem. B* **2023**, *127*, 6241−6250.
(9) Michaels, T. C.; Šarić, A.; Habchi, J.; Chia, S.; Meisl, G.; Vendruscolo, M.; Dobson, C. M.; Knowles, T. P. Chemical Kinetics for Bridging Molecular Mechanisms and Macroscopic Measurements of Amyloid Fibril Formation. *Annu. Rev. Phys. Chem.* **2018**, *69*, 273−298.
(10) Almeida, Z. L.; Brito, R. M. M. Structure and Aggregation Mechanisms in Amyloids. *Molecules* **2020**, *25*, 1195.
(11) Hnath, B.; Chen, J.; Reynolds, J.; Choi, E.; Wang, J.; Zhang, D.; Sha, C. M.; Dokholyan, N. V. Big versus small: The impact of aggregate size in disease. *Protein Sci.* **2023**, *32*, e4686.
(12) Whitfield, J. F.; Rennie, K.; Chakravarthy, B. Alzheimer's Disease and Its Possible Evolutionary Origin: Hypothesis. *Cells* **2023**, *12*, 1618.
(13) Ilie, I. M.; Caflisch, A. Simulation Studies of Amyloidogenic Polypeptides and Their Aggregates. *Chem. Rev.* **2019**, *119*, 6956−6993.
(14) Williams-Noonan, B. J.; Kamboukos, A.; Todorova, N.; Yarovsky, I. Self-assembling peptide biomaterials: Insights from spontaneous and enhanced sampling molecular dynamics simulations. *Chem. Phys. Rev.* **2023**, *4*, 021304.
(15) Eisenberg, D. S.; Sawaya, M. R. Structural Studies of Amyloid Proteins at the Molecular Level. *Annu. Rev. Biochem.* **2017**, *86*, 69−95.
(16) Narayanan, C.; Dias, C. L. Hydrophobic interactions and hydrogen bonds in β-sheet formation. *J. Chem. Phys.* **2013**, *139*, 115103.
(17) Wang, F.; Gnewou, O.; Wang, S.; Osinski, T.; Zuo, X.; Egelman, E. H.; Conticello, V. P. Deterministic chaos in the self-assembly of β sheet nanotubes from an amphipathic oligopeptide. *Matter* **2021**, *4*, 3217−3231.

https://doi.org/10.1021/acs.jpcb.3c07861
J. Phys. Chem. B XXXX, XXX, XXX−XXX

(18) Nick, M.; Wu, Y.; Schmidt, N. W.; Prusiner, S. B.; Stöhr, J.; DeGrado, W. F. A long-lived Aβ oligomer resistant to fibrillization. *Biopolymers* **2018**, *109*, e23096.
(19) Muschol, M.; Hoyer, W. Amyloid oligomers as on-pathway precursors or off-pathway competitors of fibrils. *Front. Mol. Biosci.* **2023**, *10*, 1120416.
(20) Strodel, B. Amyloid aggregation simulations: challenges, advances and perspectives. *Curr. Opin. Struct. Biol.* **2021**, *67*, 145−152.
(21) Jalali, S.; Yang, Y.; Mahmoudinobar, F.; Singh, S. M.; Nilsson, B. L.; Dias, C. Using all-atom simulations in explicit solvent to study aggregation of amphipathic peptides into amyloid-like fibrils. *J. Mol. Liq.* **2022**, *347*, 118283.
(22) Samantray, S.; Yin, F.; Kav, B.; Strodel, B. Different Force Fields Give Rise to Different Amyloid Aggregation Pathways in Molecular Dynamics Simulations. *J. Chem. Inf. Model.* **2020**, *60*, 6462−6475.
(23) Hampel, H.; Hardy, J.; Blennow, K.; Chen, C.; Perry, G.; Kim, S. H.; Villemagne, V. L.; Aisen, P.; Vendruscolo, M.; Iwatsubo, T.; et al. The Amyloid-β Pathway in Alzheimer's Disease. *Molecular Psychiatry* **2021**, *26*, 5481−5503.
(24) Stanković, I. M.; Niu, S.; Hall, M. B.; Zarić, S. D. Role of aromatic amino acids in amyloid self-assembly. *Int. J. Biol. Macromol.* **2020**, *156*, 949−959.
(25) Janković, P.; Šantek, I.; Pina, A. S.; Kalafatovic, D. Exploiting Peptide Self-Assembly for the Development of Minimalistic Viral Mimetics. *Frontiers in Chemistry* **2021**, *9*, 723473.
(26) Zhang, S.; Holmes, T.; Lockshin, C.; Rich, A. Spontaneous assembly of a self-complementary oligopeptide to form a stable macroscopic membrane. *Proc. Natl. Acad. Sci. U. S. A.* **1993**, *90*, 3334−3338.
(27) Marini, D. M.; Hwang, W.; Lauffenburger, D. A.; Zhang, S.; Kamm, R. D. Left-Handed Helical Ribbon Intermediates in the Self-Assembly of a β-Sheet Peptide. *Nano Lett.* **2002**, *2*, 295−299.
(28) Yokoi, H.; Kinoshita, T.; Zhang, S. Dynamic reassembly of peptide RADA16 nanofiber scaffold. *Proc. Natl. Acad. Sci. U. S. A.* **2005**, *102*, 8414−8419.
(29) Fändrich, M.; Fletcher, M. A.; Dobson, C. M. Amyloid fibrils from muscle myoglobin. *Nature* **2001**, *410*, 165−166.
(30) Muschol, M.; Hoyer, W. Amyloid oligomers as on-pathway precursors or off-pathway competitors of fibrils. *Front. Mol. Biosci.* **2023**, *10*, 1120416.
(31) Barz, B.; Urbanc, B. Minimal model of self-assembly: Emergence of diversity and complexity. *J. Phys. Chem. B* **2014**, *118*, 3761−3770.
(32) Maurer-Stroh, S.; Debulpaep, M.; Kuemmerer, N.; de la Paz, M. L.; Martins, I. C.; Reumers, J.; Morris, K. L.; Copland, A.; Serpell, L.; Serrano, L.; et al. Exploring the sequence determinants of amyloid structure using position-specific scoring matrices. *Nat. Methods* **2010**, *7*, 237−242.
(33) Szulc, N.; Burdukiewicz, M.; Gasior-Głogowska, M.; Wojciechowski, J. W.; Chilimoniuk, J.; Mackiewicz, P.; Šneideris, T.; Smirnovas, V.; Kotulska, M. Bioinformatics methods for identification of amyloidogenic peptides show robustness to misannotated training data. *Sci. Rep.* **2021**, *11*, 8934.
(34) Roland, B. P.; Kodali, R.; Mishra, R.; Wetzel, R. A serendipitous survey of prediction algorithms for amyloidogenicity. *Peptide Science* **2013**, *100*, 780−789.
(35) Do, T. D.; Economou, N. J.; LaPointe, N. E.; Kincannon, W. M.; Bleiholder, C.; Feinstein, S. C.; Teplow, D. B.; Buratto, S. K.; Bowers, M. T. Factors That Drive Peptide Assembly and Fibril Formation: Experimental and Theoretical Analysis of Sup35 NNQQNY Mutants. *J. Phys. Chem. B* **2013**, *117*, 8436−8446.
(36) Lee, N. R.; Bowerman, C. J.; Nilsson, B. L. Effects of Varied Sequence Pattern on the Self-Assembly of Amphipathic Peptides. *Biomacromolecules* **2013**, *14*, 3267−3277.
(37) Tornquist, M.; Michaels, T. C. T.; Sanagavarapu, K.; Yang, X.; Meisl, G.; Cohen, S. I. A.; Knowles, T. P. J.; Linse, S. Secondary nucleation in amyloid formation. *Chem. Commun.* **2018**, *54*, 8667−8684.
(38) Xue, C.; Lin, T. Y.; Chang, D.; Guo, Z. Thioflavin T as an amyloid dye: fibril quantification, optimal concentration and effect on aggregation. *Royal Society Open Science* **2017**, *4*, 160696.
(39) Tiiman, A.; Krishtal, J.; Palumaa, P.; Tõugu, V. In vitro fibrillization of Alzheimer's amyloid-β peptide (1−42). *AIP Adv.* **2015**, *5*, 092401.
(40) Nguyen, P. H.; Ramamoorthy, A.; Sahoo, B. R.; Zheng, J.; Faller, P.; Straub, J. E.; Dominguez, L.; Shea, J.-E.; Dokholyan, N. V.; De Simone, A.; et al. Amyloid Oligomers: A Joint Experimental/Computational Perspective on Alzheimer's Disease, Parkinson's Disease, Type II Diabetes, and Amyotrophic Lateral Sclerosis. *Chem. Rev.* **2021**, *121*, 2545−2647.
(41) Hsieh, M.-C.; Lynn, D. G.; Grover, M. A. Kinetic Model for Two-Step Nucleation of Peptide Assembly. *J. Phys. Chem. B* **2017**, *121*, 7401−7411.
(42) Tang, X.; Han, W. Multiscale Exploration of Concentration-Dependent Amyloid-β(16−21) Amyloid Nucleation. *J. Phys. Chem. Lett.* **2022**, *13*, 5009−5016.
(43) Young, L. J.; Kaminski Schierle, G. S.; Kaminski, C. F. Imaging Aβ(1−42) fibril elongation reveals strongly polarised growth and growth incompetent states. *Phys. Chem. Chem. Phys.* **2017**, *19*, 27987−27996.
(44) Schmit, J. D. Kinetic theory of amyloid fibril templating. *J. Chem. Phys.* **2013**, *138*, 185102.
(45) Wetzel, R. Kinetics and Thermodynamics of Amyloid Fibril Assembly. *Acc. Chem. Res.* **2006**, *39*, 671−679.
(46) Powers, E. T.; Powers, D. L. The Kinetics of Nucleated Polymerizations at High Concentrations: Amyloid Fibril Formation Near and Above the "Supercritical Concentration. *Biophys. J.* **2006**, *91*, 122−132.
(47) Michaels, T. C. T.; Saric, A.; Curk, S.; Bernfur, K.; Arosio, P.; Meisl, G.; Dear, A. J.; Cohen, S. I. A.; Dobson, C. M.; Vendruscolo, M.; et al. Dynamics of oligomer populations formed during the aggregation of Alzheimer's Aβ42 peptide. *Nat. Chem.* **2020**, *12*, 445−451.
(48) Karthika, S.; Radhakrishnan, T. K.; Kalaichelvi, P. A Review of Classical and Nonclassical Nucleation Theories. *Cryst. Growth Des.* **2016**, *16*, 6663−6681.
(49) Meisl, G.; Kirkegaard, J. B.; Arosio, P.; Michaels, T. C. T.; Vendruscolo, M.; Dobson, C. M.; Linse, S.; Knowles, T. P. J. Molecular mechanisms of protein aggregation from global fitting of kinetic models. *Nat. Protoc.* **2016**, *11*, 252−272.
(50) Yamazaki, M.; Ikeda, K.; Kameda, T.; Nakao, H.; Nakano, M. Kinetic Mechanism of Amyloid-β-(16−22) Peptide Fibrillation. *J. Phys. Chem. Lett.* **2022**, *13*, 6031−6036.
(51) Cohen, S. I. A.; Linse, S.; Luheshi, L. M.; Hellstrand, E.; White, D. A.; Rajah, L.; Otzen, D. E.; Vendruscolo, M.; Dobson, C. M.; Knowles, T. P. J. Proliferation of amyloid-β42 aggregates occurs through a secondary nucleation mechanism. *Proc. Natl. Acad. Sci. U. S. A.* **2013**, *110*, 9758−9763.
(52) Zimmermann, M. R.; Bera, S. C.; Meisl, G.; Dasadhikari, S.; Ghosh, S.; Linse, S.; Garai, K.; Knowles, T. P. J. Mechanism of Secondary Nucleation at the Single Fibril Level from Direct Observations of Aβ42 Aggregation. *J. Am. Chem. Soc.* **2021**, *143*, 16621−16629.
(53) Linse, S.; Scheidt, T.; Bernfur, K.; Vendruscolo, M.; Dobson, C. M.; Cohen, S. I. A.; Sileikis, E.; Lundqvist, M.; Qian, F.; O'Malley, T.; et al. Kinetic fingerprints differentiate the mechanisms of action of anti-Aβ antibodies. *Nature Structural & Molecular Biology* **2020**, *27*, 1125−1133.
(54) Sgourakis, N. G.; Merced-Serrano, M.; Boutsidis, C.; Drineas, P.; Du, Z.; Wang, C.; Garcia, A. E. Atomic-level characterization of the ensemble of the Aβ (1−42) monomer in water using unbiased molecular dynamics simulations and spectral algorithms. *Journal of molecular biology* **2011**, *405*, 570−583.
(55) Rosenman, D. J.; Wang, C.; García, A. E. Characterization of Aβ monomers through the convergence of ensemble properties

https://doi.org/10.1021/acs.jpcb.3c07861
J. Phys. Chem. B XXXX, XXX, XXX−XXX

among simulations with multiple force fields. *J. Phys. Chem. B* **2016**, *120*, 259−277.
(56) Mahmoudinobar, F.; Nilsson, B. L.; Dias, C. L. Effects of Ions and Small Compounds on the Structure of Aβ42 Monomers. *J. Phys. Chem. B* **2021**, *125*, 1085−1097.
(57) Carballo-Pacheco, M.; Strodel, B. Comparison of force fields for Alzheimer's A: A case study for intrinsically disordered proteins. *Protein science* **2017**, *26*, 174−185.
(58) Han, W.; Wu, Y.-D. A Strand-Loop-Strand Structure Is a Possible Intermediate in Fibril Elongation: Long Time Simulations of Amyloid-β Peptide (10- 35). *J. Am. Chem. Soc.* **2005**, *127*, 15408−15416.
(59) Khaled, M.; Rönnbäck, I.; Ilag, L. L.; Gräslund, A.; Strodel, B.; Österlund, N. A Hairpin Motif in the Amyloid-β Peptide Is Important for Formation of Disease-Related Oligomers. *J. Am. Chem. Soc.* **2023**, *145*, 18340−18354.
(60) Han, W.; Schulten, K. Fibril elongation by Aβ17−42: Kinetic network analysis of hybrid-resolution molecular dynamics simulations. *J. Am. Chem. Soc.* **2014**, *136*, 12450−12460.
(61) Hoyer, W.; Grönwall, C.; Jonsson, A.; Ståhl, S.; Härd, T. Stabilization of a β-hairpin in monomeric Alzheimer's amyloid-β peptide inhibits amyloid formation. *Proc. Natl. Acad. Sci. U. S. A.* **2008**, *105*, 5099−5104.
(62) Cao, Y.; Jiang, X.; Han, W. Self-assembly pathways of β-sheet-rich amyloid-β (1−40) dimers: Markov state model analysis on millisecond hybrid-resolution simulations. *J. Chem. Theory Comput.* **2017**, *13*, 5731−5744.
(63) Chen, M.; Schafer, N. P.; Wolynes, P. G. Surveying the energy landscapes of Aβ fibril polymorphism. *J. Phys. Chem. B* **2018**, *122*, 11414−11430.
(64) Smorodina, E.; Kav, B.; Fatafta, H.; Strodel, B. Effects of ion type and concentration on the structure and aggregation of the amyloid peptide A β 16- 22 β _16−22. *Proteins: Struct., Funct., Bioinf.* **2023**, 1−14.
(65) Jalali, S.; Zhang, R.; Haataja, M. P.; Dias, C. L. Nucleation and Growth of Amyloid Fibrils. *J. Phys. Chem. B* **2023**, *127*, 9759−9770.
(66) Zhang, R.; Jalali, S.; Dias, C. L.; Haataja, M. P. Growth kinetics of amyloid-like fibrils: An integrated atomistic simulation and continuum theory approach. *PNAS Nexus* **2024**, 045.
(67) John, T.; Rampioni, A.; Poger, D.; Mark, A. E. Molecular Insights into the Dynamics of Amyloid Fibril Growth: Elongation and Lateral Assembly of GNNQQNY Protofibrils. *ACS Chem. Neurosci.* **2024**, *15*, 716.
(68) Wei, G.; Mousseau, N.; Derreumaux, P. Sampling the Self-Assembly Pathways of KFFE Hexamers. *Biophys. J.* **2004**, *87*, 3648−3656.
(69) Cao, Y.; Tang, X.; Yuan, M.; Han, W. In *Progress in Molecular Biology and Translational Science*; Strodel, B., Barz, B., Eds.; Computational Approaches for Understanding Dynamical Systems: Protein Folding and Assembly; Academic Press, 2020; Vol. *170*, pp 461−504.
(70) Schwierz, N.; Frost, C. V.; Geissler, P. L.; Zacharias, M. Dynamics of Seeded Aβ40-Fibril Growth from Atomistic Molecular Dynamics Simulations: Kinetic Trapping and Reduced Water Mobility in the Locking Step. *J. Am. Chem. Soc.* **2016**, *138*, 527−539.
(71) Jia, Z.; Schmit, J. D.; Chen, J. Amyloid assembly is dominated by misregistered kinetic traps on an unbiased energy landscape. *Proc. Natl. Acad. Sci. U. S. A.* **2020**, *117*, 10322−10328.
(72) Schwierz, N.; Frost, C. V.; Geissler, P. L.; Zacharias, M. From Aβ Filament to Fibril: Molecular Mechanism of Surface-Activated Secondary Nucleation from All-Atom MD Simulations. *J. Phys. Chem. B* **2017**, *121*, 671−682.
(73) Bunce, S. J.; Wang, Y.; Stewart, K. L.; Ashcroft, A. E.; Radford, S. E.; Hall, C. K.; Wilson, A. J. Molecular insights into the surface-catalyzed secondary nucleation of amyloid-β40 (Aβ40) by the peptide fragment Aβ16−22. *Sci. Adv.* **2019**, *5*, eaav8216.
(74) Barz, B.; Strodel, B. Understanding Amyloid-β Oligomerization at the Molecular Level: The Role of the Fibril Surface. *Chem. Eur. J.* **2016**, *22*, 8768−8772.
(75) Petti, M. K.; Lomont, J. P.; Maj, M.; Zanni, M. T. Two-Dimensional Spectroscopy Is Being Used to Address Core Scientific Questions in Biology and Materials Science. *J. Phys. Chem. B* **2018**, *122*, 1771−1780.
(76) Andrews, B.; Guerra, J.; Schweitzer-Stenner, R.; Urbanc, B. Do molecular dynamics force fields accurately model Ramachandran distributions of amino acid residues in water? *Phys. Chem. Chem. Phys.* **2022**, *24*, 3259−3279.
(77) Schweitzer-Stenner, R.; Kurbaj, R.; O'Neill, N.; Andrews, B.; Shah, R.; Urbanc, B. Conformational Manifold Sampled by Two Short Linear Motif Segments Probed by Circular Dichroism, Vibrational, and Nuclear Magnetic Resonance Spectroscopy. *Biochemistry* **2023**, *62*, 2571−2586.
(78) Huang, J.; Rauscher, S.; Nawrocki, G.; Ran, T.; Feig, M.; De Groot, B. L.; Grubmüller, H.; MacKerell Jr, A. D. CHARMM36m: an improved force field for folded and intrinsically disordered proteins. *Nat. Methods* **2017**, *14*, 71−73.
(79) Charest, N.; Tro, M.; Bowers, M. T.; Shea, J.-E. Latent Models of Molecular Dynamics Data: Automatic Order Parameter Generation for Peptide Fibrillization. *J. Phys. Chem. B* **2020**, *124*, 8012−8022.
(80) Pretti, E.; Shell, M. S. Mapping the configurational landscape and aggregation phase behavior of the tau protein fragment PHF6. *Proc. Natl. Acad. Sci. U. S. A.* **2023**, *120*, e2309995120.
(81) Nguyen, P. H.; Derreumaux, P. Multistep molecular mechanisms of Aβ16−22 fibril formation revealed by lattice Monte Carlo simulations. *J. Chem. Phys.* **2023**, *158*, 235101.
(82) Iorio, A.; Timr, Š.; Chiodo, L.; Derreumaux, P.; Sterpone, F. Evolution of large A β 16−22 aggregates at atomic details and potential of mean force associated to peptide unbinding and fragmentation events. *Proteins: Struct., Funct., Bioinf.* **2023**, *91*, 1152−1162.
(83) Wang, Y.; Bunce, S. J.; Radford, S. E.; Wilson, A. J.; Auer, S.; Hall, C. K. Thermodynamic phase diagram of amyloid-β (16−22) peptide. *Proc. Natl. Acad. Sci. U. S. A.* **2019**, *116*, 2091−2096.
(84) Santuz, H.; Nguyen, P. H.; Sterpone, F.; Derreumaux, P. Small oligomers of Aβ42 protein in the bulk solution with AlphaFold2. *ACS Chem. Neurosci.* **2022**, *13*, 711−713.

https://doi.org/10.1021/acs.jpcb.3c07861
J. Phys. Chem. B XXXX, XXX, XXX−XXX